References

1 MARTÍN-NEIRA, M., and GOUTOULE, J.M.: 'MIRAS – a two-dimensional aperture-synthesis radiometer for soil-moisture and ocean salinity observations', *ESA Bull.*, 1997, (92), pp. 95–104

2 SIVESTRIN, P., BERGER, M., KERR, Y., and FONT, J.: 'ESA's Second Earth Explorer Opportunity Mission: The Soil Moisture and Ocean Salinity Mission – SMOS', *IEEE Geosci. Remote Sens. Newsl.*, 2001, (118), pp. 11–14

3 CAMPS, A., BARÁ, J., CORBELLA, I., and TORRES, F.: 'The processing of hexagonally sampled signals with standard rectangular techniques: application to 2D large aperture synthesis interferometric radiometers', *IEEE Trans. Geosci. Remote Sens.* GRS-35, 1997, pp. 183–190

4 BARÁ, J., CAMPS, A., TORRES, F., and CORBELLA, I.: 'Angular resolution of two-dimensional hexagonally sampled interferometric radiometer', *Radio Sci.*, 1998, **33**, (5), pp. 1459–1473

5 VALL-LLOSSERA, M., DUFFO, N., CAMPS, A., CORBELLA, I., TORRES, F., and BARÁ, J.: 'Reliability analysis in aperture synthesis interferometric radiometers: application to L-band MIRAS instrument', *Radio Sci.*, 2001, **36**, (1), pp. 107–117

SAR interferometric phase statistics in wavelet domain

C. López and X. Fàbregas

Synthetic aperture radar (SAR) interferometry is employed to obtain topographic information. Owing to noise, interferometric information has to be filtered. The wavelet transform can be employed to filter the interferometric phase, maintaining the spatial resolution, but new signal models have to be studied in this domain for further processing.

Introduction: Synthetic aperture radar interferometry (InSAR) is an established technique to obtain information about the earth's surface topography. The interferometric phase is calculated as the phase difference between two complex SAR images from the same area, but taken from slightly different positions. Owing to the lack of interferometric coherence $|\gamma|$ between both SAR images, the interferometric phase is noisy. In addition, the interferometric phase is only known within the interval $[-\pi, \pi)$, it being necessary to unwrap it to recover unambiguously the height information. The unwrapping process is also affected by phase noise, since it induces phase residues. Phase filtering is thus necessary to reduce noise effects.

In the last decade, the wavelet transform (WT) has shown a big potential for image processing applications. In the field of SAR data processing, the use of the WT is emerging since it allows processing of SAR imagery, keeping the spatial resolution and image details.

Since the physics behind SAR data is completely different from that of optical images, any data processing has to take this into account. Thus, it is necessary to review or even to define new noise models adapted to this problem. In this Letter, we provide a study of a signal model for the interferometric phase in the wavelet domain. This model is validated with real interferometric data.

Complex interferometric phase noise model: Earth topography can be represented locally by a constant slope [1], thus the interferometric phase ϕ_x can be assumed to be a constant phase ramp. In the spatial domain the measured interferometric phase complies with the model $\phi_z = \phi_x + v$ [2], where v is a phase noise term. The real and imaginary parts of the measured phase ϕ_z coded in the unit circle, defined as the complex interferometric phase, can be modelled by [3, 4]:

$$\cos(\phi_z) = N_c \cos(\phi_x) + v_c \qquad (1)$$

$$\sin(\phi_z) = N_c \sin(\phi_x) + v_s \qquad (2)$$

the wavelet transforms of which are [3]:

$$\mu_1 = DWT_{2D}\{\cos(\phi_z)\} = 2^i N_c \cos(\phi_x^w) + v_c^w \qquad (3)$$

$$\mu_2 = DWT_{2D}\{\sin(\phi_z)\} = 2^i N_c \sin(\phi_x^w) + v_s^w \qquad (4)$$

where i represents the wavelet scale. v_c^w and v_s^w are noise terms independent from the wavelet scale. The phase term ϕ_x^w represents the interferometric phase in the wavelet domain, which contains the same information as ϕ_x. The WT is able to localise ϕ_x in the space-frequency plane. N_c has a one-to-one relation with the coherence $|\gamma|$ providing, thus, the same information [3, 4].

For a constant interferometric phase and homogeneous noise (i.e. constant $|\gamma|$), the parameter N_c, as well as the terms $\cos(\phi_x^w)$ and $\sin(\phi_x^w)$ are constant. Therefore, signal randomness is only due to v_c^w and v_s^w. The discrete wavelet transform (DWT) can be seen as the addition of (weighted) random variables. By the central limit theorem, the weighted sum of identically distributed random variables can be approximated by a Gaussian distribution. Therefore, v_c^w and v_s^w are approximately Gaussian distributed. To test it, avoiding any interference from the phase ϕ_x^w, a constant slope producing 20 pixel fringes, corrupted with a noise equivalent to a coherence $|\gamma| = 0.6$, has been simulated. Table 1 shows a statistical test applied over the real part of the interferometric complex phase in the wavelet domain. As shown, since the useful signal is concentrated in the low frequency band (LL), the wavelet bands (HL, LH and HH) present a kurtosis close to 3 and the significance levels for the Kolmogorov-Smirnov (KS) test, assuming a Gaussian distribution, are high. These results demonstrate that v_c^w and v_s^w can be described by a Gaussian distribution. The same agreement is observed for any other value of $|\gamma|$, and for the imaginary part of the complex interferometric phase in the wavelet domain. The LL band deserves special attention. In this case, as there is signal content, the signal model will be represented by the real and imaginary parts of $\exp(j\phi_x^w)$ plus a Gaussian noise. Therefore, in this case, the amplitude $|\mu_1 + j\mu_2|$ has a Rice distribution. This result is equally valid for the rest of the wavelet bands. The amplitude in the wavelet domain will be Rayleigh distributed for $|\gamma| = 0$, in a particular space-frequency region, and Rice distributed for $|\gamma| > 0$

Table 1: Kurtosis and KS significance levels (Gaussian assumption) for real part of simulated complex interferometric phase ramp in wavelet domain

	Horizontal band (HL)		Vertical band (LH)		Diagonal band (LL)	
	Kurtosis	KS significance level (%)	Kurtosis	KS significance level (%)	Kurtosis	KS significance level (%)
Scale 1	2.98	87.93	2.98	79.83	2.94	98.34
Scale 2	3.03	95.78	2.97	86.08	3.00	66.15
Scale 3	3.08	82.87	2.95	85.32	3.00	82.87

Complex interferometric phase signal model: The topographic model assumed previously (i.e. constant slope) does not take into account spatial details, which are important, for instance, in urban areas. Since no information is available about the distribution of the 'true' topographic phase ϕ_x, an *a priori* model for the spatial details is not available in the spatial domain. This drawback can be overcome in the wavelet domain. As mentioned in the preceding Section, the DWT can be interpreted as a weighted sum of random variables. Therefore, $DWT_{2D}\{N_c \cos(\phi_x)\}$ and $DWT_{2D}\{N_c \sin(\phi_x)\}$ can be supposed to be determined, as a first approximation, by a Gaussian distribution. Tests with real data (see Tables 2 and 3) show that wavelet statistics have kurtosis higher than 3. To take into account this deviation from Gaussian behaviour, a double stochastic model is proposed for the wavelet coefficients x:

$$p_x(x) = \int_0^\infty p_x(x\,|_{\sigma^2}) p_{\sigma^2}(\sigma^2) d\sigma^2 \qquad (5)$$

where $p_x(x|_{\sigma^2})$ represents the Gaussian distribution of the wavelet coefficients and $p_{\sigma^2}(\sigma^2)$ is a generalised gamma distribution (GGD) modelling the variability of the variance through the phase image. $p_x(x)$ cannot be obtained in a general form. Numerical integration of (5), see Fig. 1, indicates that $p_x(x)$ can be assumed to be a GGD model. To test the validity of this model, two real interferometric phase images taken with the German sensor E-SAR from DLR have been employed. The first image is an X-band interferogram of Mount Etna (Italy) and the second one is an L-band interferogram of the Oberpfaffenhoffen test site (Germany), were man-made structures are present. These two interferometric phases were filtered with the algorithm presented in [3], which is based on maintaining the spatial resolution. Tables 2 and 3 present the kurtosis and the KS test significance levels, assuming a GGD model, applied to the real part of the filtered complex interferometric phase in the wavelet domain. These results show that the GGD model is well adapted to real data. Tables 2 and 3 also show that the Oberpfaffenhofen image presents higher kurtosis values. This result is explained by the fact that this image contains more spatial details (as buildings or roads) than the Mount Etna image, which contains only topographic information.

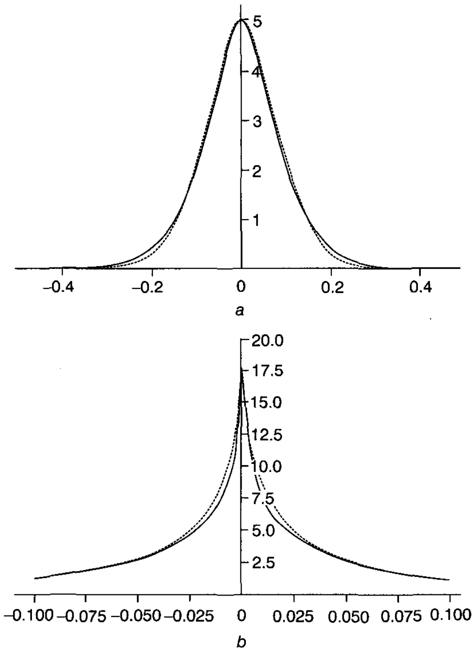

Fig. 1 *Distribution comparison between GGD model and numerical integration of double stochastic model*

a Low kurtosis
b High kurtosis
– – – GGD model
—— double stochastic model

Table 2: Kurtosis and KS significance levels (GGD assumption) for real part of Mount Etna complex interferometric phase in wavelet domain.

	Horizontal band (HL)		Vertical band (LH)		Diagonal band (HH)	
	Kurtosis	KS significance level (%)	Kurtosis	KS significance level (%)	Kurtosis	KS significance level (%)
Scale 1	10.51	70.61	11.30	77.16	12.88	56.61
Scale 2	6.39	86.51	6.42	79.89	6.12	98.33
Scale 3	4.42	97.34	5.62	60.95	3.92	80.70

Table 3: Kurtosis and KS significance levels (GGD assumption) for real part of Oberpfaffenhofen complex interferometric phase in wavelet domain.

	Horizontal band (HL)		Vertical band (LH)		Diagonal band (LL)	
	Kurtosis	KS significance level (%)	Kurtosis	KS significance level (%)	Kurtosis	KS significance level (%)
Scale 1	22.50	10.53	21.44	31.14	26.95	14.76
Scale 2	13.82	16.24	11.51	53.28	12.68	91.26
Scale 3	9.25	85.52	13.09	37.32	8.56	11.75

Conclusions: We have developed a stochastic model for the complex interferometric phase in the wavelet domain. In the first part of this Letter, assuming the topography locally as a constant slope, a reference signal model is proposed and validated. To increase its flexibility, a double stochastic signal model, which leads to a GGD model, is tested for the wavelet coefficients. In the wavelet domain, complex phase noise is Gaussian distributed, whereas the useful signal complies with a GGD model. The GGD assumption for wavelet coefficients agrees with observations reported by other researchers. Finally, this representation can be employed as *a priori* information for further processing inside the wavelet domain.

Acknowledgments: This work was funded by the Spanish government in the CICYT project TIC1999-1050-C03-01 and the Catalonian government in a DURSI fellowship.

27 July 2002
Electronics Letters Online No: 20020820
DOI: 10.1049/el:20020820

C. López and X. Fàbregas (*Signal Theory and Communications Department, Electromagnetics & Photonics Engineering Group, Universitat Politècnica de Catalunya (UPC), Building D3 Room 118, Jordi Girona 1–3, E-08034 Barcelona, Spain*)

E-mail: lopez@tsc.upc.es

References

1 GATELLI, F., GUARNERI, A.M., PARIZZI, F., PASQUALI, P., PRATI, C., and ROCCA, F.: 'The wavenumber shift in SAR interferometry', *IEEE Trans. Geosci. Remote Sens.*, 1994, **32**, (4), pp. 855–865
2 LEE, J.S., PAPATHANASSIOU, K.P., AINSWORTH, T.L., GRUNES, M.R., and REIGBER, A.: 'A new technique for noise filtering of SAR interferometric phase images', *IEEE Trans. Geosci. Remote Sens.*, 1998, **36**, (5), pp. 1456–1465
3 LÓPEZ-MARTÍNEZ, C., and FÀBREGAS-CÀNOVAS, F.X.: 'Modeling and reduction of SAR interferometric phase noise in the wavelet domain', *Accepted for publication IEEE Trans. Geosci. Remote Sens.*, 2001
4 LÓPEZ MARTÍNEZ, C., and FÀBREGAS CÀNOVAS, X.: 'Results on SAR interferometric phase noise reduction using wavelet transform'. EUSAR'02, Cologne, Germany, 2002, Vol. 1

Adaptive array antenna based on radial basis function network as multiuser detection for WCDMA

Chang-Jun Ahn and Iwao Sasase

An adaptive array antenna is proposed based on the radial basis function (RBF) network as a multiuser detector for a WCDMA system. The proposed system calculates the optimal combining weight coefficients using sample matrix inversion with a common correlation matrix algorithm and obtains the channel response vector using the RBF output signal.

Introduction: Wideband code division multiple access (WCDMA) communication systems have recently attracted considerable attention as mobile cellular and IMT-2000 communication systems due to their ability to suppress a wide variety of interfering signals including narrowband interference, multiple access interference (MAI), and multipath interference (MPI). One of the approaches for improving WCDMA system performance is the use of spatial filtering at a base station with an adaptive antenna array. The adaptive array antenna is widely accepted, since it provides many promising features such as high capacity, high spectrum efficiency, and more degrees of freedom to adjust cell coverage characteristics, leading to more efficient use of radio resources. To obtain the optimal combining weight coefficients used in this technique, several adaptive algorithms such as the sample matrix inversion (SMI) and least mean square (LMS) algorithm have been proposed. In array antennas using these conventional algorithms, weight processing is individually carried out for each user. Therefore, the base station must have many independent weight processors, which increase computational complexity. To solve this problem, a sample matrix inversion with a common correlation matrix (CCM-SMI) has been proposed. This algorithm has low computational complexity, fast weight convergence, and good BER performance at the base station in a multiuser environment. However, the CCM-SMI-based adaptive array antenna system has a poor channel response vector (as does SMI) due to the active multiuser. Since the MF output signal includes MAI with increasing users, the system